

# Hydrogen bond dynamics at the glass transition

U. Buchenau\*

*Forschungszentrum Jülich GmbH, Jülich Centre for Neutron Science (JCNS-1)  
and Institute for Complex Systems (ICS-1), 52425 Jülich, GERMANY*

(Dated: August 19, 2021)

The glass transition in hydrogen-bonded glass formers differs from the glass transition in other glass formers. The Eshelby rearrangements of the highly viscous flow are superimposed by strongly asymmetric hydrogen bond rupture processes, responsible for the excess wing. Their influence on the shear relaxation spectrum is strong in glycerol and close to zero in PPE, reflecting the strength of the hydrogen bond contribution to the high frequency shear modulus. An appropriate modification of a recent theory of the highly viscous flow enables a quantitative common description of the relaxation spectra in shear, linear and non-linear dielectrics, and heat capacity.

PACS numbers: 78.35.+c, 63.50.Lm

At the glass transition [1–4], hydrogen bonds [5, 6] have specific dynamics, always at the beginning and sometimes also at the end of the flow process: at long times, in the monoalcohols [7], the hydrogen bond decay is a Debye process, with a relaxation time much longer than the terminal shear relaxation time  $\tau_c$ , so the hydrogen bond connection memory can survive the breakdown of rigidity, similar to the case of polymers [8].

At short times, two peculiarities seem to appear exclusively in hydrogen-bonded glass formers, namely strongly asymmetric double-well potentials in the recoverable part of the flow relaxation [9, 10] and the excess wing at very short relaxation times [10–12]. Both features have very recently been shown to be absent in several non-hydrogen-bonding glass formers by combining mechanical data in the glass phase at many different frequencies from the literature [13].

The first clear evidence for strongly asymmetric double-well potentials in hydrogen-bonded substances appeared in an aging experiment [9]. An average asymmetry of  $3.8 k_B T_g$  is needed to explain the intensity rise of the strong secondary relaxation peak dielectric signal in tripropylene glycol immediately after the initial temperature jump.

The second proof for a strong asymmetry is the strong temperature dependence  $\exp(5T/T_g)$  of the excess wing measured in the glass phase of glycerol and other hydrogen bonded glass formers [10], explainable in terms of the asymmetry  $\Delta = 5k_B T_g$ , leading to the weakening factor  $1/\cosh(\Delta/2k_B T)^2 \approx \exp(5(T - 1.52T_g)/T_g)$  for  $T$  slightly below  $T_g$ .

The present paper argues that the process behind these strongly asymmetric double-well potentials is the reversible rupture of hydrogen bonds.

The breaking of hydrogen bonds has been intensely studied in liquid water, in the water shell of biomolecules [14, 15] and at the glass transition of water-chlorine mixtures [16]. In liquid water at room temperature, a hydro-

gen bond between two water molecules has two lifetimes, a short reversible one of 0.5 ps, after which it breaks, links to another water molecule, but then returns to its former state, and a longer irreversible one of 6.5 ps [14]. Both processes are visible in the dielectric spectrum of water [17, 18], the short time process accounting for about 10 % of the total decay. Obviously, this short time process is a rupture and re-formation of the hydrogen bond leading to a metastable energy minimum lying higher than the initial one, with a high back-jump probability, precisely the kind of process needed to understand the strongly asymmetric double-well potentials in the recoverable compliance of hydrogen-bonded glass formers.

The fact that the flow relaxation in all glass formers consists of a recoverable and an irreversible part is nowadays often overlooked [1–4], but has been established unambiguously long ago by the centennial shear relaxation work of Donald Plazek [19–22]. In the shear relaxation, the irreversible part is described by the viscosity  $\eta$ . The reversible part consists of a Kohlrausch tail  $t^\beta$  ( $t$  time,  $\beta$  Kohlrausch exponent) of the recoverable shear compliance at times shorter than the terminal relaxation time  $\tau_c$  of the viscous flow. Plazek favors the Andrade value  $\beta = 1/3$ . But his data do not establish  $\beta$  with high accuracy; more extensive investigations [23, 24] find a wide distribution of  $\beta$  values around 1/2.

A theoretical analysis of the reversible and irreversible shear transformation processes in the five-dimensional shear space [25–27] in terms of asymmetric double-well potentials, with the asymmetry determined exclusively by the different shear misfit of the inner Eshelby domain [28] or shear transformation zone [29, 30] in its two structural alternatives, leads to the relaxation time distribution in the barrier variable  $v = \ln(\tau/\tau_c)$

$$l_{irrev}(v) = \frac{1}{3\sqrt{2\pi}} \exp(v^2) \left( \ln(4\sqrt{2}) - v \right)^{3/2} \quad (1)$$

for the irreversible processes, with  $\tau_c = 8\eta/G$  ( $G$  short time shear modulus). Note that the spectrum has no Kohlrausch tail at short times; it is more like a slightly broadened Debye process around the relaxation time 1.6  $\tau_c$ , a factor of thirteen longer than the Maxwell time.

\*Electronic address: buchenau-juelich@t-online.de

The spectrum is able to reproduce [27] a high quality measurement [31] of the terminal stage of the aging process in squalane, with  $\tau_c$  extrapolated from shear data in the liquid phase.

This irreversible process spectrum describes dynamic heat capacity data not only in a metallic glass, but also in three hydrogen bonding substances, the vacuum pump oil PPE, glycerol and propylene glycol [25, 26], with  $\tau_c$  determined from shear relaxation data of the same substances. Obviously, the additional asymmetric processes in these substances do not change the validity of eq. (1) for the irreversible flow processes. Since the irreversible processes are a continuation of the Eshelby processes of the Kohlrausch tail to relaxation times longer than  $\tau_c$ , this implies that there must be a basic Kohlrausch tail in the hydrogen-bonded substances identical to the one in other glass formers.

But what obviously happens is that the basic Kohlrausch tail relaxations combine with a reversible hydrogen bond rupture, creating a double well potential with a strong additional asymmetry. This effect is bound to become stronger as the Kohlrausch tail approaches from above barrier energies close to the local hydrogen bond barriers of about 0.1 eV suggested by the picosecond scale of the hydrogen bond motion in water [14]. This is the physical reason for the excess wing and its flattening in the nanosecond region.

How does this modify the basic Kohlrausch tail? The strengthening toward lower barriers adds a logarithmic curvature, so the tail has to be described in terms of a Kohlrausch barrier density  $\exp(\beta(v + f_{exc}v^2))$ , with a small excess wing parameter  $f_{exc}$ . The second necessary change has been already seen in the first attempt to fit hydrogen bonding spectra in terms of the theory [26]: because of the higher back-jump probability, one needs a higher Kohlrausch barrier density to achieve the viscous flow, describable in terms of a prefactor  $f_K > 1$  for the Kohlrausch tail. Together, these two effects modify the theoretical equation [27] into

$$l_K(v) = f_K(1 + 0.115\beta - 1.18\beta^2)F(v) \exp(\beta(v + f_{exc}v^2)). \quad (2)$$

Here  $F(v) \approx 1/(1 + \exp(1.19v))$  is the cutoff function of the Kohlrausch tail by the irreversible processes [27].

Having defined  $l_K(v)$ , one can calculate the complex shear compliance  $J(\omega)$  from

$$GJ(\omega) = 1 + \int_{-\infty}^{\infty} \frac{l_K(v)dv}{1 + i\omega\tau_c \exp(v)} - \frac{i}{\omega\tau_M}, \quad (3)$$

where  $\tau_M = \eta/G = \tau_c/8$  is the Maxwell time, and invert it to get  $G(\omega)$ .

Fig. 1 (a) shows the fit of the shear relaxation data [32] in glycerol at 196 K in terms of these equations, with the parameters compiled in Table I, demonstrating that the postulate of an additional slow mode [32] is not the only way to understand these data.

As pointed out in the theoretical paper [27], the simultaneous knowledge of irreversible and reversible relax-

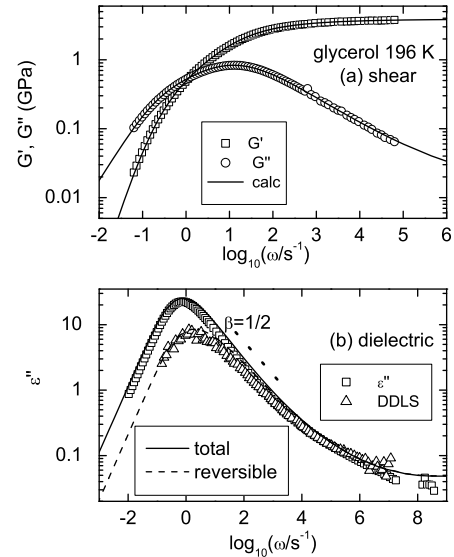


FIG. 1: (a) Measurement [32] of  $G(\omega)$  in glycerol, continuous lines calculated with the parameters in Table I (b) Fit of dielectric data [33] at the same temperature with the parameters in Table II. The dashed line is calculated without the irreversible processes and happens to provide a good description of the depolarized dynamic light scattering data [11] (but see also Supplemental Material).

subst.	$T$ K	$G$ GPa	$\eta$ GPAs	$\beta$	$f_K$	$f_{exc}$	$GJ_0$
glycerol	196	3.93	1.80	0.65	5.95	0.014	11.2
propylene carbonate	159	1.47	0.523	0.51	1.47	0.009	4.26
PPE	250	1.09	0.725	0.48	1	0	3.03
propylene glycol	180	4.05	0.17	0.68	5.17	0.021	10.0

TABLE I: Parameters for the theoretical description of shear relaxation data (references see text) in the four hydrogen-bonded glass formers (PPE=5-polyphenylene ether).

ation processes from the shear data implies the knowledge of all Eshelby shear relaxation processes of the substance, and enables one to judge what one sees in other relaxation techniques. The application of this concept to dielectric and adiabatic compressibility data in non-hydrogen-bonded glass formers revealed that the scheme works very well, but the dielectric and compressibility signals required the multiplication of the total spectrum with  $\exp(-\tau/\tau_t)$ , where  $\tau_t$  is a terminal time shorter than  $\tau_c$ , showing that the dielectric polarizability and the adiabatic compressibility equilibrate earlier than the terminal shear relaxation time.

In the application of the scheme to dielectric and depolarized dynamic light scattering in hydrogen bonded substances, one must multiply also the irreversible contribution of eq. (1) with  $f_K$ , because otherwise there is a discontinuity in the barrier density at  $\tau_c$ . The resulting Eshelby barrier density is

$$l_E(v) = 8f_K l_{irrev}(v) + l_K(v) \exp(-\exp(v)/\tau_t). \quad (4)$$

The Debye peak in the monoalcohols [7] suggests to add a hydrogen-bond-correlation Debye decay at the time  $\tau_t$

$$l_{tot}(v) = l_D \delta(v - \ln(\tau_t/\tau_c)) + l_0 l_E(v), \quad (5)$$

where  $l_0$  normalizes  $l_E(v)$  to  $1 - l_D$ .

Fig. 1 (b) shows that one can describe the dielectric spectrum [33] with this recipe. However, one must adapt the excess wing parameter  $f_{exc}$ , which is a bit larger in the dielectric data. As a consequence, one must also adapt  $\beta$  to a slightly higher value, because the slope of the Kohlrausch tail at  $\tau_c$  contains a small negative component from the diminishing influence of hydrogen bonds toward higher barriers. The five parameters  $\Delta\chi$  (the difference between the dielectric susceptibilities at very low and very high frequency),  $f_{exc}$ ,  $\tau_t/\tau_c$ ,  $\beta$  and  $l_D$  for the dielectric data are listed in Table II.

subst.	$T$ K	$\Delta\chi$	$\beta$	$f_{exc}$	$\tau_t/\tau_c$	$l_D$
glycerol	196	62.7	0.71	0.018	0.51	0.21
propylene carbonate	159	101.0	0.67	0.019	1.55	0.29
PPE	250	1.9	0.63	0.014	0.83	0.10
propylene glycol	180	64.4	0.68	0.021	81.0	0.00

TABLE II: Parameters for the theoretical description of dielectric relaxation data (references see text) in the four hydrogen-bonded glass formers.

Fig. 1 (b) shows also, as a dashed line, the calculated dielectric signal without the irreversible processes, which happens to describe the shifted depolarized dynamic light scattering data [11] very well. However, as argued by Thomas Blochowicz (see Supplemental Material), this agreement can be shown to be fortuitous.

Glycerol with its three strong oxygen hydrogen bonds per molecule has a much higher shear modulus than propylene carbonate, where the oxygen atoms do not have a hydrogen atom of their own, but link to the hydrogens bonded to carbon atoms. As a consequence, the deviation of the parameter  $f_K$  from 1 in Table I of propylene carbonate is about a factor of ten smaller than the one of glycerol, and its shear modulus is not much higher than the 1 GPa of van-der-Waals bonded molecular glass formers [26]. But otherwise, the results of the same analysis of propylene carbonate data [34] shown in Fig. 2 (a) and (b) and tabulated in Table I and II are very similar.

PPE has even weaker hydrogen bonds, so weak that one gets a perfect fit of the shear data [35] in terms of the original model with only the three parameters  $G$ ,  $\eta$  and  $\beta$  in Table I, taken over from [27]. But the former fit of the dielectric data [27] improves markedly with the parameters of Table II, as demonstrated in Fig. 3. The excess wing parameter is about the same as in the other three substances and  $\beta$  changes strongly, showing that the dielectric signal is dominated by the strong hydrogen bond component which is not visible in the shear data.

The last example, propylene glycol, has again a strong hydrogen bond component in its shear data [36]. In the

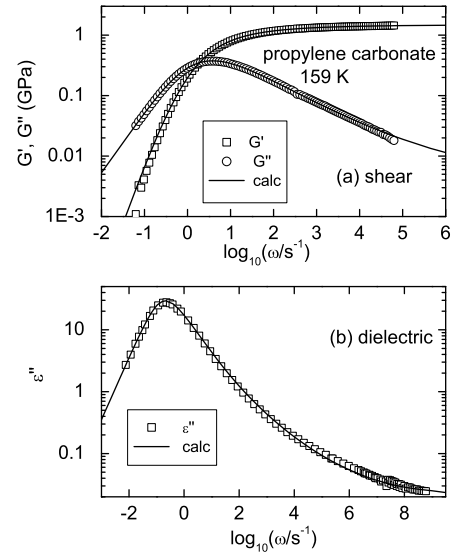


FIG. 2: (a) Measurement [34] of  $G(\omega)$  in propylene carbonate at 159 K, continuous lines calculated with the parameters in Table I (b) Fit of dielectric data [34] at the same temperature in the same cryostat with the parameters in Table II.

dielectric data [37], one finds the same  $f_{exc}$  and  $\beta$  as in the shear data. In this case, one does not really need  $\tau_t$ ; the dielectric relaxation terminates at the value calculated from the shear data and there is no hydrogen-bond-correlation Debye decay within experimental error.

The description of dielectric data of hydrogen-bonded glass formers in terms of strongly asymmetric double-well potentials supplies a new interpretation of nonlinear dielectric data (see Supplemental Material).

Table I compiles the parameters for the four substances, including in the last row the total recoverable compliance  $GJ_0$ , which in glycerol is nearly a factor of four higher than in normal glass formers, showing that one needs much more recoverable processes to start the viscous flow, because of the strong back-jump tendency of the hydrogen bonds. In all four cases, the shear analysis was done over the entire temperature range of the

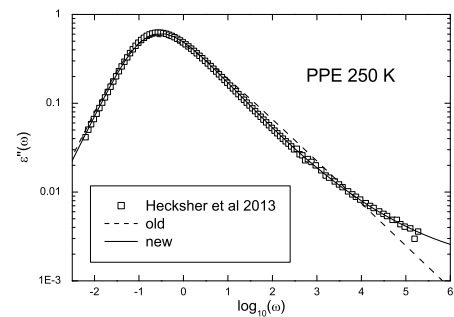


FIG. 3: (Old [27] (dashed line) and new (continuous line, parameters Table II) calculations for dielectric data in PPE at 250 K [35].

measurements, to look for a possible temperature dependence of the parameters.  $f_K$  and  $f_{exc}$  were found to be temperature-independent within experimental accuracy. For glycerol, the temperature-dependent shear moduli agree within a few percent with those of a transverse wave Brillouin scattering determination [38], showing the high quality of both measurements.

Though one has to invoke a stronger asymmetry, the possibility to obtain good fits of high quality shear data in hydrogen bonding substances with the two additional parameters  $f_K$  for the strength of the hydrogen bond influence and  $f_{exc}$  for the excess wing curvature supports the validity of the general theory of the highly viscous

flow [27].

To summarize, one can understand the shear relaxation of hydrogen-bonded undercooled liquids close to their glass transition in a recent theory of the highly viscous flow by taking the influence of highly asymmetric reversible hydrogen bond ruptures, well studied in water, into account. The hydrogen bond ruptures make the Kohlrausch tail double-well potentials strongly asymmetric and give rise to the excess wing, absent in non-hydrogen-bonded glass formers. One can describe shear, linear and non-linear dielectric, and dynamic specific heat data consistently within the extended theory.

---

[1] A. Cavagna, *Phys. Rep.* **476**, 51 (2009)

[2] L. Berthier and G. Biroli, *Rev. Mod. Phys.* **83**, 587 (2011)

[3] C. P. Royall and S. R. Williams, *Phys. Rep.* **560**, 1 (2015)

[4] L. Berthier, *J. Chem. Phys.* **150**, 160902 (2019)

[5] Th. Steiner, *Angew. Chem. Int. Ed.* **41**, 48 (2002)

[6] V. David, N. Grinberg, and S. C. Moldoveanu, in *Advances in Chromatography Vol. 54* (Eds: E. Gruschka, N. Grinberg), CRC, Boca Raton 2018, chap. 3

[7] R. Böhmer, C. Gainaru', and R. Richert, *Phys. Rep.* **545**, 125 (2014)

[8] A. L. Agapov, V. N. Novikov, T. Hong, F. Fan, and A. P. Sokolov, *Macromolecules* **51**, 4874 (2018)

[9] J. C. Dyre and N. B. Olsen, *Phys. Rev. Lett.* **91**, 155703 (2003)

[10] C. Gainaru, R. Böhmer, R. Kahlau, and E. Rössler, *Phys. Rev. B* **82**, 104205 (2010)

[11] J. Ph. Gabriel, P. Zourchang, F. Pabst, A. Helbling, P. Weigl, T. Böhmer, and Th. Blochowicz, *Phys.Chem.Chem.Phys.* **22**, 11644 (2020)

[12] F. Pabst, J. Gabriel, T. Böhmer, P. Weigl, A. Helbling, T. Richter, P. Zourchang, Th. Walther, and Th. Blochowicz, *arXiv:2008.01021*

[13] U. Buchenau, G. D'Angelo, G. Carini, X. Liu, and M. A. Ramos, *arXiv:2012.10139*

[14] B. Bagchi, *Chem. Rev.* **105**, 3197 (2003)

[15] D. Laage and J. T. Hynes, *Science* **311**, 832 (2006)

[16] D. Corradini, M. Rovere, and P. Gallo, *J. Chem. Phys.* **132**, 134508 (2010)

[17] J. B. Hasted, S. K. Husain, F. A. M. Frescura, and R. Birch, *Chem. Phys. Lett.* **118**, 622 (1985)

[18] W. J. Ellison, K. Lamakaouchi, and J.-M. Moreau, *J. Mol. Liq.* **68**, 171 (1996)

[19] D. J. Plazek, *J. Phys. Chem.* **69**, 3480 (1965)

[20] D. J. Plazek and J. H. Magill, *J. Chem. Phys.* **45**, 3038 (1966)

[21] D. J. Plazek, C. A. Bero and I.-C. Chay, *J. Non-Cryst. Solids* **172-174**, 181 (1994)

[22] C. M. Roland, P. G. Santangelo, D. J. Plazek, and K. M. Bernatz, *J. Chem. Phys.* **111**, 9337 (1999)

[23] R. Böhmer, K. L. Ngai, C. A. Angell and D. J. Plazek, *J. Phys. Chem.* **99**, 4201 (1993)

[24] A. I. Nielsen, T. Christensen, B. Jakobsen, K. Niss, N. B. Olsen, R. Richert, and J. C. Dyre, *J. Chem. Phys.* **130**, 154508 (2009)

[25] U. Buchenau, *J. Chem. Phys.* **148**, 064502 (2018)

[26] U. Buchenau, *J. Chem. Phys.* **149**, 044508 (2018)

[27] U. Buchenau, *arXiv:2003.07246*

[28] J. D. Eshelby, *Proc. Roy. Soc. A* **241**, 376 (1957)

[29] M. L. Falk and J. S. Langer, *Phys. Rev. E* **57**, 7192 (1998)

[30] W. L. Johnson and K. Samwer, *Phys. Rev. Lett.* **95**, 195501 (2005)

[31] K. Niss, J. C. Dyre, and T. Hecksher, *J. Chem. Phys.* **152**, 041103 (2020)

[32] M. H. Jensen, C. Gainaru, C. Alba-Simionescu, T. Hecksher, and K. Niss, *Phys. Chem. Chem. Phys.* **20**, 1716 (2018)

[33] S. Adichtchev, T. Blochowicz, C. Tschirwitz, V. N. Novikov and E. A. Rössler, *Phys. Rev. E* **68**, 011504 (2003)

[34] C. Gainaru, T. Hecksher, N. B. Olsen, R. Böhmer, and J. C. Dyre, *J. Chem. Phys.* **137**, 064508 (2012)

[35] T. Hecksher, N. B. Olsen, K. A. Nelson, J. C. Dyre and T. Christensen, *J. Chem. Phys.* **138**, 12A543 (2013)

[36] C. Maggi, B. Jakobsen, T. Christensen, N. B. Olsen and J. C. Dyre, *J. Phys. Chem. B* **112**, 16320 (2008)

[37] C. Leon, K. L. Ngai, and C. M. Roland, *J. Chem. Phys.* **110**, 11585 (1999)

[38] F. Scarponi, L. Comez, D. Fioretto, and L. Palmieri, *Phys. Rev. B* **70**, 054203 (2004)

# Supplemental Material: Hydrogen bond dynamics at the glass transition

U. Buchenau\*

*Forschungszentrum Jülich GmbH, Jülich Centre for Neutron Science (JCNS-1)  
and Institute for Complex Systems (ICS-1), 52425 Jülich, GERMANY*

(Dated: August 19, 2021)

The argument of Thomas Blochowicz for the depolarized dynamical scattering is presented and discussed. The consequences of the main paper for the nonlinear dielectric effects are worked out.

PACS numbers: 78.35.+c, 63.50.Lm

## I. DEPOLARIZED DYNAMICAL LIGHT SCATTERING: BLOCHOWICZ ARGUMENT

The imaginary peak of the depolarized dynamical light scattering data in glycerol lies a factor of three higher than the one of the dielectric data [1]. In an earlier draft [2] of the present paper, this led to the hypothesis that one sees only reversible relaxations in the depolarized dynamical light scattering.

In a discussion with the Author, Thomas Blochowicz pointed out that one could check the hypothesis in DC704, where the two peaks happen to coincide [3].

This is done in Fig. 1, which shows the dielectric spectrum [4] of DC704 and its fitted [5] full and reversible parts, with a reversible part peak frequency a factor of 2.5 higher than the one of the full spectrum.

The comparison to the measured depolarized dynamical light scattering data of DC704 [3] shows clearly that the hypothesis is wrong. In fact, the hypothesis has the additional weakness that, according to theory [6], at the crossover from reversible to irreversible structural transitions their nature does not change, so their visibility in the depolarized dynamic light scattering should not change.

Looking for an alternative explanation of the upwards peak shift from dielectrics to depolarized dynamical light scattering in glycerol, one remembers that for the simple case of isotropic rotational diffusion of a molecular dipole Debye [7] predicts the peak in  $\epsilon''$  at  $\omega = 2D_r$  ( $D_r$  rotational diffusion constant) and Berne and Pecora [8] predict the imaginary peak in the depolarized dynamical light scattering at  $\omega = 6D_r$ , a factor of three higher.

Naturally, the molecular motion in the  $\alpha$ -relaxation of glycerol is not a simple rotational diffusion. On the other hand, the terminal stage of the motion at the time  $\tau_t$ , where the many Eshelby transitions in which the molecule participated have removed its initial connection to its neighbors, is essentially a small-angle motion according to NMR evidence [9]. So the measured peak shift in glycerol [1] seems understandable, even quantitatively.

But this poses the question why the peak shift is not observed in DC704 [3].

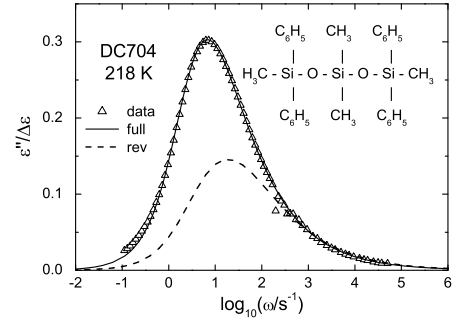


FIG. 1: Dielectric data [4] in DC704 at 218 K, together with their theoretical fit [5] (continuous line). Taking only the reversible processes to be responsible for the depolarized dynamical light scattering, one predicts the dashed line with a peak shift which is not observed in experiment [3]. The structure of DC704 with its two Si-O-Si bonds in the center is shown in the upper right side of the figure.

To understand this, look at the structure of the DC704 molecule in Fig. 1, with its two very flexible Si-O-Si bond bending degrees of freedom. The dipole moment of each of them is given by the displacement of the oxygen atom from the line connecting the two silicon atoms. One does not expect the very large DC704 molecule to rotate much during the whole  $\alpha$ -process, but the Si-O-Si dipole moments will change in every Eshelby transition in which the molecule participates. If one idealizes each Si-O-Si bond as a dipole making large jumps in a fixed plane perpendicular to the line connecting the two silicon atoms, with a 180-degree jump equally probable as a 90-degree jump, one does indeed predict equal peak positions in dielectrics and depolarized dynamical light scattering.

## II. NONLINEAR DIELECTRIC EFFECTS

The first two decades of this century have provided high quality experimental nonlinear dielectric results, all of them taken close to the glass transition in hydrogen-bonded undercooled liquids [10–24]. These data hold the promise for a deep insight into the nature of the highly viscous flow - if one could understand them.

Previous attempts [17, 25] to explain the experimental findings in terms of the nonlinear dielectric response of

\*Electronic address: buchenau-juelich@t-online.de

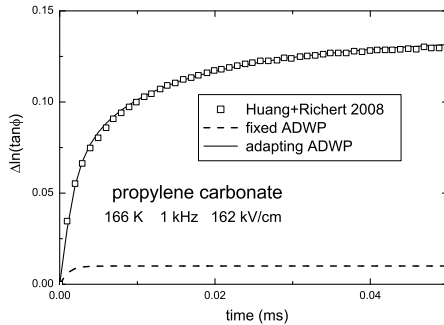


FIG. 2: Fit of nonlinear dielectric absorption data in propylene carbonate after switching on a strong alternating electric field [13] in terms of relaxations in asymmetric double-well potentials with a time-dependent asymmetry (see text).

asymmetric double-well potentials [17, 26] were not very successful, but Ranko Richert's phenomenological model [10, 12–14, 16, 23], sometimes also called box model, is impressively able to explain all nonlinear dielectric findings without any free parameter. The model requires the hole-burning assumption [27] that the relaxations heat up into a different state when they absorb the electric energy.

The results of the present paper enable a new interpretation of the Richert model in terms of asymmetric double-well potentials. This is demonstrated in Fig. 2 for the saturation of the nonlinear absorption after switching on a strong alternating electric field, measured for many substances by Richert and coworkers [13, 14, 16]. Fig. 2 shows the example of propylene carbonate, where the effect is very strong [12, 13, 16], measured at 1 kHz, a frequency about fifty times higher than the peak in  $\epsilon''(\omega)$ .

According to the present paper, one has asymmetric double-well potentials at this frequency, with a lifetime which is much longer than their relaxation time. The two wells are Eshelby regions with different structures, and the strength of the nonlinear dielectric signal is determined by the dipole moment change  $M$  and the asymmetry  $\Delta$  of the Eshelby transition [17, 26]. In a strong alternating electric field, the population of the upper well increases, the more so the higher the asymmetry  $\Delta$  is. After switching on the strong alternating field, the nonlinear effect should saturate with the relaxation time of the potentials which one sees, essentially with  $f_\omega(t) = 1 - \exp(-\omega t)$  (the dashed curve in Fig. 2).

While the initial slope of the measured nonlinear part  $\Delta \ln \Phi$  of the phase shift is found [14] to be proportional to  $\omega$ , showing that one deals indeed with relaxations around  $\omega\tau = 1$ , the saturation goes much slower than expected for a time-independent asymmetric double-well potential, with the terminal relaxation time of the dynamical heat capacity, suggesting the slow change of the relaxation within its lifetime postulated in the Richert model.

Here, it is assumed that the nonlinear higher occupation of the higher well causes the surroundings to adapt to the higher elastic misfit of the upper well, thus diminishing the asymmetry and increasing the oscillating dipole moment. According to the present paper, the appropriate Kohlrausch saturation function for such a change is  $f_K(t) = 1 - \exp((-t/1.6\tau_c)^\beta)$ , taking  $\tau_c$  and  $\beta$  from dynamical shear data. Then

$$\Delta \ln \Phi(t) = 0.01 f_\omega(t) + 0.129 f_\omega(t) f_K(t), \quad (1)$$

the continuous line in Fig. 2, where the two factors 0.01 and 0.129 were fitted to the data. In  $f_K(t)$ ,  $\tau_c$  at 166 K is 4.2 ms, and  $\beta = 0.52$  from the dynamic shear data [28].

Within this picture, the adaptation of the asymmetric double-well potentials to the field-induced population increase of the upper well increases the nonlinear response at the frequency  $\omega$  by a large Richert factor  $f_R$ , in propylene carbonate by  $f_R = 12.9$ . There is no increase of the dipole moment change  $M$  of the Eshelby transition, but a decrease of the asymmetry  $\Delta$ , leading to a small increase of its prefactor  $1/\cosh^2(\Delta/2k_B T)$ . Thus it is rather a linear effect, only with a driving force which increases quadratically with the electric field amplitude. This explains why the slow part of the increase of Fig. 2 is only seen at  $\omega$ , while the nonlinear effect at  $3\omega$  remains constant and is small [13], consistent with the small first component of eq. (1).

One can use this interpretation to construct a strongly simplified description of the nonlinear spectra, adding the

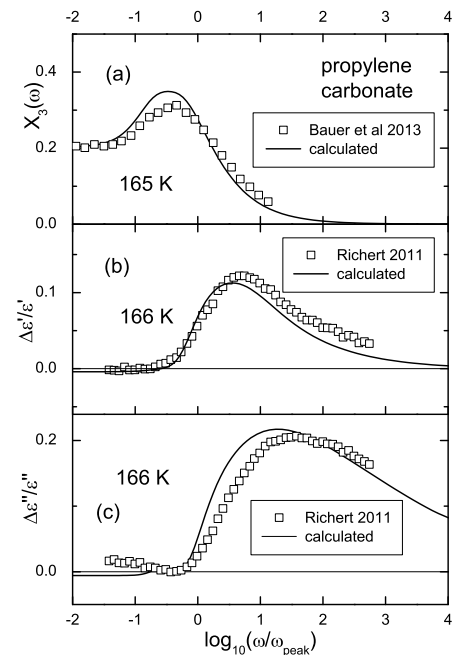


FIG. 3: Fit of nonlinear effects in propylene carbonate as a function of frequency in terms of the asymmetric double-well potential model (a)  $3\omega$ -data [20] (b)  $\Delta\epsilon'/\epsilon'$ -data at a field of 177 kV/cm [16] (c)  $\Delta\epsilon''/\epsilon''$ -data at a field of 177 kV/cm [16].

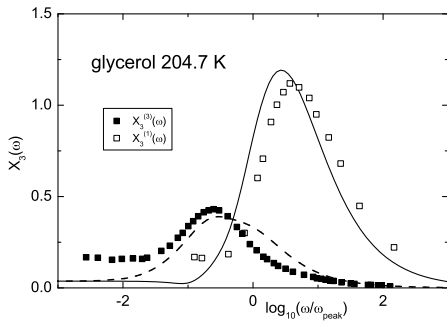


FIG. 4: Fit of nonlinear data in glycerol [17] as a function of frequency in terms of the asymmetric double-well potential model.

Langevin saturation of the molecular dipole moment  $\mu$  at longer times to the nonlinear Eshelby transition effects at shorter times. To do this, one notes first that the adaptation effect, which dominates the nonlinear  $\omega$ -response at higher frequency, does not lead to any change at very low frequency, where the electric field is practically constant within the lifetime of an Eshelby region.

Another central question is how the finite lifetime  $\tau_E$  of the Eshelby regions affects the nonlinear response of the asymmetric double-well potential [17, 26] for a strong alternating electric field at the frequency  $\omega$ . The effect can obviously be neglected for high frequencies with  $\omega\tau_E \gg 1$ .

Here, it is argued that it can also be neglected for  $\omega\tau_E \ll 1$ . The long-time nonlinear contribution of a symmetric double-well potential is negative, for the same saturation reason as for a freely reorienting dipole, and changes sign [26] at  $\delta^2 = 1/3$ , where  $\delta = \tanh(\Delta/2k_B T)$ . This long-time nonlinear signal remains unchanged if the potential is newly created from time to time. Thus the Eshelby transitions provide a positive nonlinear contribution at the frequency zero for an average  $\delta^2 > 1/3$  and a negative contribution in the opposite case.

To take the lifetime influence into account, one multiplies the nonlinear signal of the asymmetric double-well potential [26] with  $1 - \exp(-1/\omega\tau_E)$  and adds its nonlinear signal at the frequency zero with the factor  $\exp(-1/\omega\tau_E)$ . In the present description

$$\frac{1}{\tau_E} = \frac{1}{1.6\tau_c} + \frac{1}{\tau_t}. \quad (2)$$

With these assumptions, and simplifying the problem further by assuming that all relevant Eshelby regions have the same  $M$  and average  $\delta^2$ , one is able to calculate the nonlinear dielectric response of a strong alternating electric field at all frequencies from eq. (5) of the main paper, inserting the parameters from Table I and II of the main paper, and fitting the three additional parameters  $M$ ,  $\delta^2$  and  $f_R$  to the nonlinear data. For a reasonable fit, one finds that one needs two additional simplifying assumptions: (1) the irreversible Eshelby transitions have the same nonlinear effects as the reversible ones (2) the

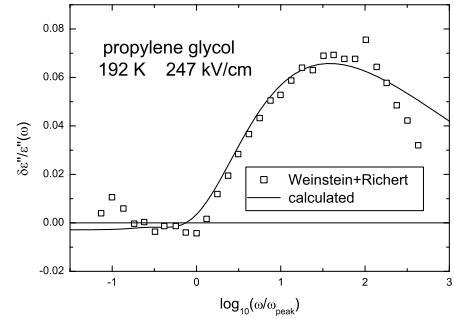


FIG. 5: Fit of  $\Delta\epsilon''/\epsilon''$  in propylene glycol [11] as a function of frequency in terms of the asymmetric double-well potential model.

excess wing has practically no nonlinear signal. The single molecule Langevin saturation is treated in terms of the nonlinear Debye solution [29], distributed over the relaxation times of the irreversible transitions.

The convention [17]  $\chi_3^{(3)}(0) = \chi_3^{(1)}(0) = \Delta\epsilon/E_e^2$  identifies the two nonlinear third order susceptibilities close to the frequency zero with the Piekara factor, which describes the change  $\Delta\epsilon$  of the susceptibility in the external electric field  $E_e$ . Inside the sample,  $E_e$  is strengthened by the Onsager factor  $f_{On} = \epsilon(n^2+2)^2/3(2\epsilon+n^2)$ , where  $n$  is the refractive index. For the linear response

$$\Delta\chi = \frac{N\mu^2 f_{On}}{3\epsilon_0 kT}, \quad (3)$$

where  $\Delta\chi$  is the susceptibility difference between high and low frequency, and  $N$  is the number density of molecules. The third order susceptibility can be expressed in a convenient dimensionless form [17]

$$X_3(\omega) = \frac{NkT}{\epsilon_0 \Delta\chi^2} |\chi_3^{(3)}(\omega)|. \quad (4)$$

Fig. 3 (a) shows the fit of the measured nonlinear susceptibility [20] of propylene carbonate at  $3\omega$ , Fig. 3 (b) and 3 (c) the fit of the measured changes  $\Delta\epsilon'/\epsilon'$  and  $\Delta\epsilon''/\epsilon''$  [16] at  $\omega$ , plotted as functions of the frequency in units of the peak frequency of  $\epsilon''(\omega)$ , with the parameters listed in Table I. Fig. 4 shows fits of glycerol data [17] and Fig. 5 of polypropylene data.

The fits show that the strong asymmetry of about  $5 k_B T_g$  of the excess wing (see main paper) is no longer found in the neighborhood of the terminal relaxation time  $\tau_c$ . In all three substances,  $\delta^2$  is close to  $1/3$ , corresponding to  $\Delta/k_B T_g = 1.317$ , where the sign of the zero frequency contribution changes. The value is still more than a factor of two higher than the  $1/2 k_B T$  expected for a single degree of freedom without external influences. In propylene glycol, the exact value of  $1/3$  for  $\delta^2$  is forced by the finding of the Piekara factor expected for the single molecule [11], excluding any influence of the Eshelby regions at the frequency zero. With this low value, the present description predicts no visible hump in the  $3\omega$

signal of propylene glycol, because it ascribes the hump to the lowering of the Piekara factor by the positive contribution of the Eshelby regions.

subst.	$T$	$\Delta\chi$	$\mu$	$M/\mu$	$\delta^2$	$f_R$
	K		D			
propylene carbonate	166	130.0	5.67	3.3	0.373	12.0
glycerol	204.7	62.7	4.26	3.9	0.377	2.9
propylene glycol	192	88.0	2.25	3.3	0.333	5.0

TABLE I: Parameters for the theoretical description of nonlinear dielectric relaxation data (references see text) in the three hydrogen-bonded glass formers.

The values  $M/\mu$  in Table I do not directly tell one the number of molecules in an Eshelby region, because  $M/\mu$  depends also on the turning angle of the hydrogen bond in a structural transition and on the percentage of hydrogen bonds which break. But  $(M/\mu)^2$  should be proportional to the number of molecules in an Eshelby region, and enters as a factor for the height of the nonlinear signal at higher frequencies. Therefore the increase of the nonlinear signals with decreasing temperature does in-

deed indicate an increase of the size of the cooperatively rearranging regions responsible for the viscous flow with decreasing temperature, one of the possible explanations [17, 20] for the fragility.

The Richert factor  $f_R$  fitted to the spectra of propylene carbonate in Fig. 3 agrees within the error bars with the one determined from the absorption saturation data in Fig. 2. It is much smaller in glycerol and propylene glycol than in propylene carbonate, according to the Richert model due to the much smaller fragility [12]. Since the present modification also attributes the Richert factor to the balance between gained electric field energy and lost structural entropy, this conclusion remains valid.

One advantage of the Richert model gets lost in the present picture, namely the possibility to predict exact numbers for the nonlinear effects from the assumption that the electric field energy goes to hundred percent into a transformation of the relaxation to one corresponding to a higher temperature. The validity of this assumption does not follow in an obvious way from the asymmetric double-well potential concept described here.

---

[1] J. Ph. Gabriel, P. Zourchang, F. Pabst, A. Helbling, P. Weigl, T. Böhmer, and Th. Blochowicz, *Phys. Chem. Chem. Phys.* **22**, 11644 (2020)

[2] U. Buchenau, arXiv:2105.06394v2

[3] F. Pabst, J. Ph. Gabriel, T. Böhmer, P. Weigl, A. Helbling, T. Richter, P. Zourchang, Th. Walther, and Th. Blochowicz, *J. Phys. Chem. Lett.* **12**, 14 (2021)

[4] T. Hecksher, N. B. Olsen, K. A. Nelson, J. C. Dyre and T. Christensen, *J. Chem. Phys.* **138**, 12A543 (2013)

[5] U. Buchenau, arXiv:2003.07246

[6] U. Buchenau, *J. Chem. Phys.* **149**, 044508 (2018)

[7] P. Debye, *Polar Liquids*, Chem. Catalog Comp., N. Y. 1929

[8] B. J. Berne and R. Pecora, *Dynamic Light Scattering*, Wiley-Interscience, 1976

[9] G. Diezemann, R. Böhmer, G. Hinze, and H. Sillescu, *J. Non-Cryst. Solids* **235-237**, 121 (1998)

[10] R. Richert and S. Weinstein, *Phys. Rev. Lett.* **97**, 095703 (2006)

[11] S. Weinstein and R. Richert, *Phys. Rev. B* **75**, 064302 (2007)

[12] L.-M. Wang and R. Richert, *Phys. Rev. Lett.* **99**, 185701 (2007)

[13] W. Huang and R. Richert, *Eur. Phys. J. B* **66**, 217 (2008)

[14] W. Huang and R. Richert, *J. Chem. Phys.* **130**, 194509 (2009)

[15] C. Crauste-Thibierge, C. Brun, F. Ladieu, D. L'Hôte, G. Biroli, and J.-P. Bouchaud, *Phys. Rev. Lett.* **104**, 165703 (2010)

[16] R. Richert, *Thermochimica Acta* **522**, 28 (2011)

[17] C. Brun, F. Ladieu, D. L'Hôte, M. Tarzia, G. Biroli, and J.-P. Bouchaud, *Phys. Rev. B* **84**, 104204 (2011)

[18] F. Ladieu, C. Brun, D. L'Hôte, *Phys. Rev. B* **85**, 184207 (2012)

[19] Th. Bauer, P. Lunkenheimer, S. Kastner and A. Loidl, *Phys. Rev. Lett.* **110**, 107603 (2013)

[20] Th. Bauer, P. Lunkenheimer and A. Loidl, *Phys. Rev. Lett.* **111**, 225702 (2013)

[21] Th. Bauer, M. Michl, P. Lunkenheimer, and A. Loidl, *J. Non-Cryst. Solids* **407**, 66 (2015)

[22] S. Samanta and R. Richert, *J. Chem. Phys.* **140**, 054503 (2014)

[23] P. Kim, A. R. Young-Gonzalez, and R. Richert, *J. Chem. Phys.* **145**, 064510 (2016)

[24] S. Albert, Th. Bauer, M. Michl, G. Biroli, J.-P. Bouchaud, A. Loidl, P. Lunkenheimer, R. Tourbot, C. Wiertel-Gasquet, and F. Ladieu, *Science* **352**, 1308 (2016)

[25] U. Buchenau, *J. Chem. Phys.* **146**, 214503 (2017)

[26] G. Diezemann, *Phys. Rev. E* **85**, 051502 (2012)

[27] B. Schiener, R. Böhmer, A. Loidl, and R. V. Chamberlin, *Science* **274**, 752 (1996)

[28] C. Gainaru, T. Hecksher, N. B. Olsen, R. Böhmer, and J. C. Dyre, *J. Chem. Phys.* **137**, 064508 (2012)

[29] W. T. Coffey, B. V. Paranjape, *Proc. R. Irish Acad. A* **78**, 17 (1978)